Video Article

An Alternative Approach to Study Primary Events in Neurodegeneration Using *Ex Vivo* Rat Brain Slices

Emanuele Brai[1], Antonella Cogoni[1], Susan A. Greenfield[1]

[1]Neuro-Bio Ltd, Building F5, Culham Science Centre

Correspondence to: Emanuele Brai at emanuele.brai@neuro-bio.com

URL: https://www.jove.com/video/57507
DOI: doi:10.3791/57507

Keywords: Neuroscience, Issue 134, Neurodegeneration, Alzheimer's disease, *ex vivo* brain sections, basal forebrain, AChE-derived peptide, α7 nicotinic receptor, amyloid beta, phosphorylated Tau

Date Published: 4/12/2018

Citation: Brai, E., Cogoni, A., Greenfield, S.A. An Alternative Approach to Study Primary Events in Neurodegeneration Using *Ex Vivo* Rat Brain Slices. *J. Vis. Exp.* (134), e57507, doi:10.3791/57507 (2018).

Abstract

Despite numerous studies that attempt to develop reliable animal models which reflecting the primary processes underlying neurodegeneration, very few have been widely accepted. Here, we propose a new procedure adapted from the well-known *ex vivo* brain slice technique, which offers a closer *in vivo*-like scenario than *in vitro* preparations, for investigating the early events triggering cell degeneration, as observed in Alzheimer's disease (AD). This variation consists of simple and easily reproducible steps, which enable preservation of the anatomical cytoarchitecture of the selected brain region and its local functionality in a physiological milieu. Different anatomical areas can be obtained from the same brain, providing the opportunity to perform multiple experiments with the treatments in question in a site-, dose-, and time-dependent manner. Potential limitations which could affect the outcomes related to this methodology are related to the conservation of the tissue, *i.e.,* the maintenance of its anatomical integrity during the slicing and incubation steps and the section thickness, which can influence the biochemical and immunohistochemical analysis. This approach can be employed for different purposes, such as exploring molecular mechanisms involved in physiological or pathological conditions, drug screening, or dose-response assays. Finally, this protocol could also reduce the number of animals employed in behavioral studies. The application reported here has been recently described and tested for the first time on *ex vivo* rat brain slices containing the basal forebrain (BF), which is one of the cerebral regions primarily affected in AD. Specifically, it has been demonstrated that the administration of a toxic peptide derived from the C-terminus of acetylcholinesterase (AChE) could prompt an AD-like profile, triggering, along the antero-posterior axis of the BF, a differential expression of proteins altered in AD, such as the alpha7 nicotinic receptor (α7-nAChR), phosphorylated Tau (p-Tau), and amyloid beta (Aβ).

Video Link

The video component of this article can be found at https://www.jove.com/video/57507/

Introduction

AD is a chronic pathology characterized by gradual neurodegenerative impairment affecting different brain areas, such as the entorhinal cortex (EC), BF, hippocampus (HC), and olfactory bulb (OB)[1,2,3,4,5]. The late stages of AD development lead to a progressive cognitive decline, making this disease the most common form of dementia, approximately accounting for 70% of all cases[6]. Despite extensive attempts to understand the initial stages causing AD, there is not currently a defined experimental indication elucidating them. In addition, the most popular theory - the "amyloid hypothesis" - is increasingly questioned since it does not provide a complete profile in explaining the AD pathobiology, nor a pharmaceutical target that has proved effective[7,8,9].

An alternative theory which is receiving increasing attention suggests that the initial mechanisms occurring during neurodegeneration are related to a neuronal cluster primarily susceptible in AD[3,10,11,12,13,14]. This heterogeneous cellular hub encompassed within the BF, midbrain, and brainstem, projects to multiple regions, such as the EC, HC, and OB[15,16]. Despite its diversity in neuronal morphology and neurotransmitter synthesis, this core of cells shares a common feature in expressing AChE, which can also have a non-enzymatic function[17,18]. This non-classical role as a novel signaling molecule mediates calcium (Ca^{2+}) flow into neurons which can undergo trophic or toxic events in relation to Ca^{2+} dose, availability, and neuronal age[17,18,19].

During neurodegeneration, the observed cellular loss might be therefore associated to this non-enzymatic function[17,18,20], which is attributable to a 30mer peptide (T30) cleaved from the AChE C-terminus[20]. In line with previous results, carried on cell culture and optical imaging[18,21] preparations, we demonstrated, through a novel approach based on *ex vivo* rat brain slices containing BF structures, that T30 induced an AD-like profile[22]. Specifically, this new methodology offers a more physiological scenario than cell culture since it maintains many of the characteristics of an intact tissue, ranging from anatomical to circuitry preservation, albeit for a time window of hours. We applied this protocol to explore the events taking place during the early phases of neurodegeneration, monitoring the acute response upon T30 application.

Despite the large body of literature on using brain slices to investigate molecular pathways implied in neuronal damage or neurogenesis[23,24], this protocol provides for the first time a more immediate and sensitive read out compared to the common use of organotypic slices. However,

as is the case for organotypic brain sections, this acute slice procedure can also be adopted for several purposes, such as the evaluation of neuroprotective or neurotoxic molecules, discovery of primary molecular changes occurring in a specific process, immunohistochemical analysis, and pharmacological assays for central nervous system related pathologies.

Protocol

All animal studies have been performed under approved protocols.

NOTE: In this section, the sequence of the main phases performed during the experimental procedure and the suggested time interval is provided (**Figure 1**). Moreover, a step-by-step description of the protocol is supplemented by an illustrative panel, showing critical actions ranging from brain removal to tissue homogenization after the incubation period (**Figure 2**). The details regarding the materials and instructions to build the apparatus and the subsequent phase for the WB analysis are previously described[22].

1. Surgical Tools, Vibratome Settings and Treatment Preparation

NOTE: Execute the following steps before starting the experimental procedure:

1. Prepare two different artificial cerebrospinal fluids (aCSFs), one used for the brain slicing and the other for the incubation step as previously described[29]. Briefly, the working concentrations (in mmol) of the two aCSFs are for the "slicing" aCSF: 120 NaCl, 5 KCl, 20 $NaHCO_3$, 2.4 $CaCl_2$, 2 $MgSO_4$, 1.2 KH_2PO_4, and 10 glucose; 6.7 HEPES salt and 3.3 HEPES acid; pH: 7.1. While for the "recording" aCSF: 124 NaCl, 3.7 KCl, 26 $NaHCO_3$, 2 $CaCl_2$, 1.3 $MgSO_4$, 1.3 KH_2PO_4, and 10 glucose; pH: 7.1.
2. Mix well the solutions and then put on ice and oxygenate the slicing aCSF in order to have it cold while removing the brain and the subsequent sectioning. Keep at room temperature (RT) and supply oxygen to the recording aCSF.
3. Place the instruments under the dissection hood for the decapitation and brain removal, *i.e.*, guillotine, surgical dissection kit (scissors, forceps, blades), and spatula.
4. Set up the vibratome parameters by selecting the slice thickness (300 µm in this preparation) and the frequency at 7 and the speed at 6. Insert the vibratome chamber in its appropriate space and surround it with ice.
5. Open the carbogen (95% O_2, 5% CO_2) valve to oxygenate the "slicing" (aCSF) during the brain sectioning. Select the minimum flow rate, around 2 mL/min.
6. Take two 15-mL tubes to prepare the conditions to test. Add in one tube 10 mL of the "recording" aCSF alone (control group) and in the other, 10 mL of the "recording" aCSF enriched with T30 at a concentration of 2 µM (treated group). Vortex both tubes and keep them on ice until their use in the setup preparation phase (section 3).

2. Anesthesia, Brain Extraction and Slicing

NOTE: In this study, 9 wild type P14 male Wistar rats were used. Brain extraction and subsequent slicing constitute a critical part of the protocol since they should be quickly performed (within 10 min) in order to prevent or at least slow down tissue degeneration processes.

1. Add 1.5 mL of 100% w/w of isoflurane on a cotton layer into the induction chamber, place the animal inside, and close the lid. Wait until the animal is deeply anesthetized, confirming the absence of the pedal reflex, and then decapitate the animal using the guillotine.
2. Keep the head of the animal within a pot containing ice-cold slicing aCSF during the brain removal step (**Figure 2A - C**).
3. Incise the skin over the skull with a surgical blade, then cut the skull using scissors following the midline, from the posterior part and proceed anteriorly until reaching the bone above the OBs (**Figure 2A**).
4. Pull laterally the two sides of the skull using a pair of forceps in order to have access to the brain (**Figure 2B**). Insert a spatula ventrally to the brain, gently scoop it out, and keep it hydrated in ice-cold "slicing" aCSF for approximately 5 min (**Figure 2C**).
5. Dispose the brain on filter paper and cut out the cerebellum using a blade (**Figure 2D**). Glue the brain vertically on the vibratome disc and insert it inside the sectioning chamber, fill it with ice-cold "slicing" aCSF, and provide oxygen (**Figure 2E**).
6. Adjust the cutting interval, and proceed with the brain sectioning (**Figure 2F**). Collect the sections containing the region of interest, such as the medial septum (MS), diagonal band of Broca (DBB), and substantia innominata (SI), as previously described[22]. From top to the bottom, the three slices contain the rostral (R), intermediate (I), and caudal (C) portion of the BF (**Figure 2G**).
7. Divide along the midline each section with small scissors, obtaining two specular hemislices (**Figure 2H**), used individually as the control and treated condition at the same anatomical plane.
8. Keep the hemisections in the vibratome chamber for 5 - 10 min, then transfer them with a glass pipette into a bubbling pot containing recording aCSF. Keep at RT for approximately 30 min to recover.
9. Fill, in the meantime, three glass vials with 3 mL of recording aCSF alone (previously prepared in step 1.6) for the control group and three vials with 3 mL of aCSF enriched with T30 (previously prepared in step 1.6) for the treated group.

3. Setup Preparation

1. Transfer the hemisections into their corresponding glass vials (**Figure 2I**) in order to have three consecutive hemislices (including the rostral, intermediate, and caudal BF region) for the control group (green frame, **Figure 2J**) and their matching counterparts for the treated group (red frame, **Figure 2J**).
2. Transfer the brain tissue with two different brushes, one for the control hemislices and another for the treated counterparts, in order to prevent any contamination between conditions.
3. Seal each glass vial with the corresponding lid, presenting the oxygenating needle (21G) (**Figure 2J**). Connect the main tube of the apparatus to the carbogen source (**Figure 2K**). Deliver oxygen to the hemislices throughout the incubation period with a minimal flow rate of 2 mL/min in order to avoid any movement of the brain tissue and possible mechanical damage during the experiment. Start the 5 h incubation. Execute the steps 3.1 - 3.3 within 5 min.

NOTE: Check frequently (every 15 - 20 min) whether the oxygen is supplied into all the vials and that its flow is not moving the tissue from the bottom.

4. Sample Homogenization

1. Stop the oxygen flow after the incubation and remove all the lids from the vials. Transfer the hemislices, using the proper brushes, into 1.5 mL tubes containing 250 µL of lysis buffer, maintaining the tubes on ice (**Figure 2L**). To make the lysis buffer, mix PBS 1x with phosphatase and protease inhibitors cocktails both diluted at 1:100, and homogenize the tissue with different pestles to prevent contamination among the samples. Complete these actions within 10 - 15 min.
2. Centrifuge the brain lysate at 1,000 x g for 5 min at 4 °C. Transfer the supernatant into new tubes and keep the samples at -80 °C.

5. Reading of the Protein Concentration and Western Blot Analysis

1. Determine the protein concentration of each sample and subsequently prepare the aliquots for Western blot analysis as previously described[22].
2. Perform statistical analysis to evaluate the effects of the treatment on protein expression.

Representative Results

The protocol presented here indicates that the administration of a toxic peptide, T30, modulates in a site-dependent manner the expression of α7-nAChR, p-Tau, and Aβ in BF-containing sections (**Figure 3A**). The nicotinic receptor shows a significant increase in the rostral-treated hemislice compared to its control counterpart (slice 1, $p = 0.0310$) (**Figure 3B**), while the intermediate slice does not reveal any change between the two conditions (slice 2, $p = 0.1195$) (**Figure 3B**). In the posterior section a significant reduction is present in the T30-exposed portion over its control side (slice 3, $p = 0.0476$) (**Figure 3B**). Upon T30 application, p-Tau levels are significantly increased in the anterior region against the control matching side (slice 1, $p = 0.0158$) (**Figure 3C**). On the other hand, the other two BF-containing sections do not show any significant difference between the conditions (slice 2, $p = 0.1014$; slice 3, $p = 0.6405$) (**Figure 3C**). After T30 exposure, Aβ is significantly enhanced in the rostral and intermediate hemisections when compared to their untreated contralateral portions (slice 1, $p = 0.0136$; slice 2, $p = 0.0109$) (**Figure 3D**). In the caudal slice, there is no change between the two treatments (slice 3, $p = 0.1231$) (**Figure 3D**). The primary antibody against p-Tau recognizes the epitope containing the phosphorylated Ser202 residue. The primary antibody against Aβ detects several isoforms, ranging from Aβ37 to Aβ42. Data were analyzed as previously described[22] using two tailed paired *t*-tests and represented as SEM. N = (hemislices per group, rats) is (27, 9).

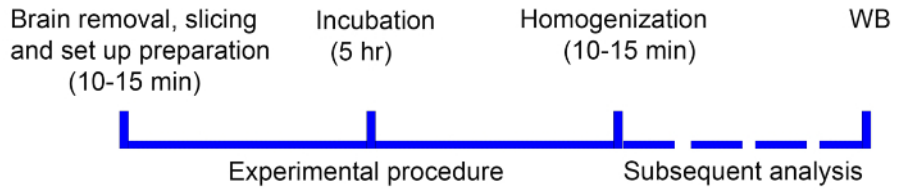

Figure 1: Sequence and indicative timing of the main steps performed during the experimental procedure. The time interval to complete the first and third step can vary in relation to the operator's experience level. Please click here to view a larger version of this figure.

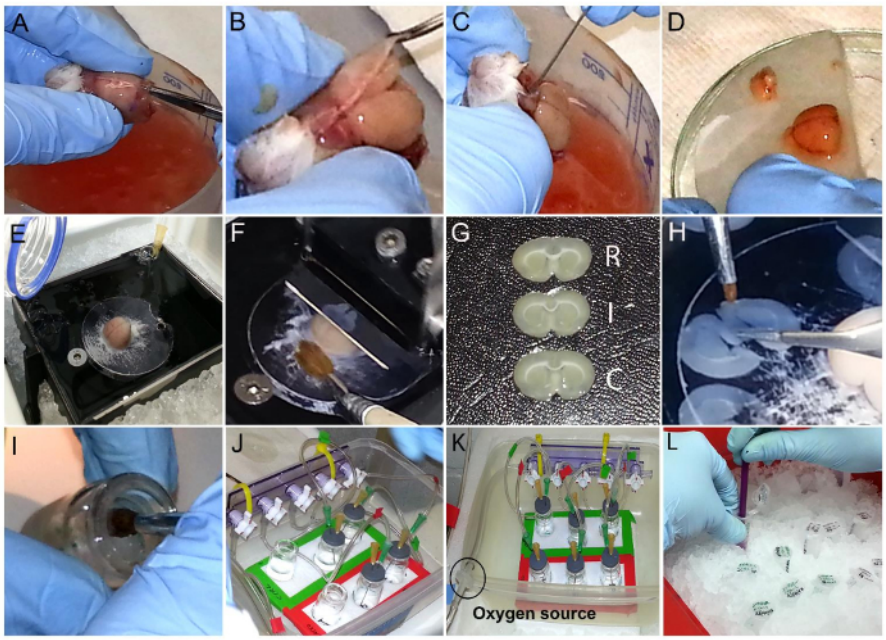

Figure 2: Sequential steps illustrating the protocol progression. (**A-D**) Extraction of the brain from the skull and separation of the cerebellum from the rest of the brain. (**E**) Attachment of the brain on the vibratome disc and transfer into the dissection chamber, which is surrounded by ice and filled with cold aCSF constantly oxygenated during the slicing. (**F**) Coronal brain sectioning. (**G**) Collection of the slices, containing rostral (**R**), intermediate (**I**), and caudal (**C**) structures of the basal forebrain. (**H**) Separation of the sections in two matching hemislices. (**I**) Each hemisection is placed into its corresponding vial. (**J**) Vials positioned in the support, inside the apparatus box and separately closed. (**K**) Incubation period upon the connection of the system to the oxygen source (black circle). (**L**) Homogenization of the samples after the treatment. This figure is modified from[22]. Please click here to view a larger version of this figure.

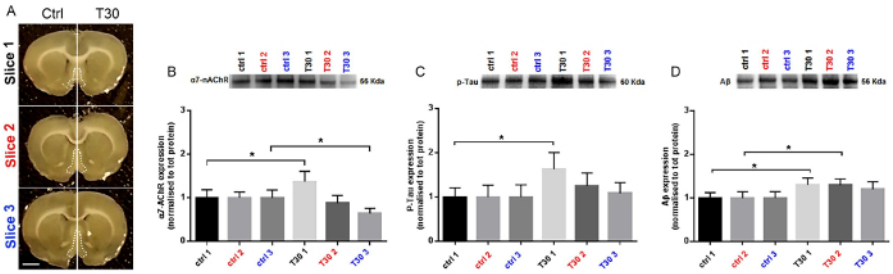

Figure 3: T30 mediated site-specific expression of α7-nAChR, p-Tau, and Aβ along the BF rostro-caudal axis. (**A**) Representation of brain coronal slices including basal forebrain nuclei (white dotted lines), divided in two complementary portions and exposed to different conditions. (**B**) After T30 exposure, the nicotinic receptor shows a significant increase in the anterior subdivision (T30 1) and a marked reduction in the posterior one (T30 3) compared to the corresponding control sides (ctrl 1 and ctrl 3). The intermediate slice does not display any change between the two conditions (ctrl 2, T30 2). (**C**) p-Tau expression is significantly higher in the treated rostral portion (T30 1) over its control matching counterpart (ctrl 1), whereas the other two slices do not reveal any difference in the two groups (slice 2 and slice 3). (**D**) Aβ displays a significant increase in the anterior and intermediate treated subdivisions (T30 1 and T30 2) compared to their corresponding untreated sides (ctrl 1 and ctrl 2). In the caudal sections, there is no variation between the two groups. The error bars indicate SEM. * p <0.05.n = (hemislices per group, rats) is (27, 9). Scale bar is 1 mm. This figure has been modified from[22]. Please click here to view a larger version of this figure.

Discussion

The principal aspect of this protocol, based on the well-established *ex vivo* brain technique, allows to synchronously test two specular hemislices, obtained from the same anatomical plane, monitoring their response after the application of a specific condition (control or treated); this therefore offers an experimental paradigm as tightly controlled as possible. The possibility of evaluating in a time-, dose-, and site-specific manner different neurochemicals related to neuronal impairment, as seen during neurodegenerative events[22], represents an essential feature. This methodology links the advantages of an *in vivo* physiological environment with those of *in vitro* preparations, such as accuracy in obtaining the region of interest and creating the ideal extracellular context. This protocol represents an adaptation of the common brain slicing procedure widely used for *ex vivo* electrophysiological recordings[25,26,27] and optical imaging[28,29,30], or *in vitro* organotypic slices, which simulate a closer *in vivo* situation by enabling the preservation of both structural and synaptic organization[23,24,31,32].

Furthermore, this procedure could help to decrease the number of animals used in behavioral studies since it partially replicates an *in vivo*-like condition, which can be adopted to confirm *in vitro* data, such as cell culture and immunohistochemical analysis, and then anticipate *in vivo* experiments.

The proposed methodology presents also some limitations, such as the section thickness and integrity which, when not appropriate, can alter the final outcome. The incubation time is also a fundamental component of this technique since it might influence the comparison between the control group and the treated one. In addition, a series of procedural or technical problems can be encountered during all the steps of the protocol, such as: (1) mechanical damage while extracting or sectioning the brain, which can be avoided by precise and gentle handling of the tissue; (2) floating of the hemislices during the incubation due to an excessive oxygen flow, which can mechanically damage the tissue if it touches the oxygenating needle submerged in the aCSF, thus affecting its integrity. This can be prevented by adjusting to the minimum rate the bubbling; and (3) absence or inconstant oxygen flow, which can be related to the empty canister, a damage or disconnection in the tubing system, a plug in the oxygenating needle, or when it is not properly immersed in the aCSF. Since the constant oxygenation and its flow throughout the procedure represents one of the most critical aspects of this protocol, it is important to frequently monitor all these parameters to maintain a homogeneous condition between the investigated groups.

Other critical steps in the protocol are represented by the time windows required to perform each action, which when followed will preserve as much as possible the integrity and functionality of the tissue. In addition, to assess these parameters, immunohistochemical analysis can be performed to detect specific markers related to neuronal viability and electrophysiological recordings as previously described[23,29].

Beyond the results described here, this method could be designed *ad hoc* for specific investigations. For instance, it can be applied to: (1) monitor and compare the activity of different compounds in several brain areas, incubating them with the selected solution, such as aCSF or Neurobasal medium; (2) perform studies on hypoxia, since the oxygen flow can be selectively controlled in each hemisection; (3) investigate brain tissue properties from transgenic animal models of different diseases; (4) simultaneously explore, at the same anatomical level, the effects of *in vivo* unilateral brain injections and compare them with the control hemisphere; and (5) explore other organs or tissues properties, therefore potentially facilitating and reducing the length of drug screening trials.

Disclosures

The authors declare competing financial interests. Susan A. Greenfield is the founder and president of Neuro-Bio Limited, a privately owned Company, and holds shares in the Company. Emanuele Brai and Antonella Cogoni are employees of Neuro-Bio Ltd.

Acknowledgements

This work was funded by Neuro-Bio Ltd. We would like to thank Dr. Giovanni Ferrati and Dr. Sergio Rotondo (Neuro-Bio) for their comments and advice on the manuscript.

References

1. Braak, H., & Braak, E. Neuropathological stageing of Alzheimer-related changes. *Acta Neuropathologica.* **82** (4), 239-259 (1991).
2. Schliebs, R. Basal forebrain cholinergic dysfunction in Alzheimer's disease--interrelationship with beta-amyloid, inflammation and neurotrophin signaling. *Neurochemical Research.* **30** (6-7), 895-908 (2005).
3. Schmitz, T. W. *et al.* Basal forebrain degeneration precedes and predicts the cortical spread of Alzheimer's pathology. *Nature Communications.* **7**, 13249 (2016).
4. Fjell, A. M., McEvoy, L., Holland, D., Dale, A. M., Walhovd, K. B., & Alzheimer's Disease Neuroimaging Initiative What is normal in normal aging? Effects of aging, amyloid and Alzheimer's disease on the cerebral cortex and the hippocampus. *Progress in neurobiology.* **117**, 20-40 (2014).
5. Kovács, T., Cairns, N. J., & Lantos, P. L. Olfactory centres in Alzheimer's disease: olfactory bulb is involved in early Braak's stages. *Neuroreport.* **12** (2), 285-288 (2001).
6. Winblad, B. *et al.* Defeating Alzheimer's disease and other dementias: a priority for European science and society. *The Lancet Neurology.* **15** (5), 455-532 (2016).
7. Herrup, K. The case for rejecting the amyloid cascade hypothesis. *Nat Neurosci.* **18** (6), 794-799 (2015).
8. De Strooper, B., & Karran, E. The Cellular Phase of Alzheimer's Disease. *Cell.* **164** (4), 603-615 (2016).
9. Scheltens, P. *et al.* Alzheimer's disease. *Lancet.* **388** (10043), 505-517 (2016).
10. Arendt, T., Brückner, M. K., Lange, M., & Bigl, V. Changes in acetylcholinesterase and butyrylcholinesterase in Alzheimer's disease resemble embryonic development-A study of molecular forms. *Neurochemistry International.* **21** (3), 381-396 (1992).
11. Auld, D. S., Kornecook, T. J., Bastianetto, S., & Quirion, R. Alzheimer's disease and the basal forebrain cholinergic system: relations to β-amyloid peptides, cognition, and treatment strategies. *Progress in Neurobiology.* **68** (3), 209-245 (2002).
12. Arendt, T., Bruckner, M. K., Morawski, M., Jager, C., & Gertz, H. J. Early neurone loss in Alzheimer's disease: cortical or subcortical? *Acta Neuropathol Commun.* **3**, 10 (2015).
13. Mesulam, M. The Cholinergic Lesion of Alzheimer's Disease: Pivotal Factor or The Cholinergic Lesion of Alzheimer's Disease: Pivotal Factor or Side Show? *Learn Mem.* 43-49 (2004).
14. Schliebs, R., & Arendt, T. The cholinergic system in aging and neuronal degeneration. *Behavioural Brain Research.* **221** (2), 555-563 (2011).
15. Mesulam, M. M., Mufson, E. J., Wainer, B. H., & Levey, A. I. Central cholinergic pathways in the rat: An overview based on an alternative nomenclature (Ch1-Ch6). *Neuroscience.* **10** (4), 1185-1201 (1983).
16. Mesulam, M., Mufson, E. J., Levey, A. I., & Wainer, B. H. Cholinergic innervation of cortex by the basal forebrain: cytochemistry and cortical connections of the septal area, diagonal band nuclei, nucleus basalis (substantia innominata), and hypothalamus in the rhesus monkey. *J Comp Neurol.* **214**(2) 170-97 (1983).
17. Greenfield, S. Discovering and targeting the basic mechanism of neurodegeneration: The role of peptides from the C-terminus of acetylcholinesterase: Non-hydrolytic effects of ache: The actions of peptides derived from the C-terminal and their relevance to neurodegenerat. *Chemico-Biological Interactions.* **203** (3), 543-546 (2013).

18. Garcia-Ratés, S. *et al.* (I) Pharmacological profiling of a novel modulator of the α7 nicotinic receptor: Blockade of a toxic acetylcholinesterase-derived peptide increased in Alzheimer brains. *Neuropharmacology.* **105**, 487-499 (2016).
19. Eimerl, S., & Schramm, M. The quantity of calcium that appears to induce neuronal death. *Journal of neurochemistry.* **62** (3), 1223-6 at <http://www.ncbi.nlm.nih.gov/pubmed/8113805> (1994).
20. Greenfield, S., & Vaux, D. J. Commentary Parkinson's Disease, Alzheimer's Disease and Motor Neurone Disease: Identifying a Common Mechanism. *Science.* **113** (3), 485-492 (2002).
21. Badin, A. S., Morrill, P., Devonshire, I. M., & Greenfield, S. A. (II) Physiological profiling of an endogenous peptide in the basal forebrain: Age-related bioactivity and blockade with a novel modulator. *Neuropharmacology.* **105**, 47-60 (2016).
22. Brai, E., Stuart, S., Badin, A.-S., & Greenfield, S. A. A Novel Ex Vivo Model to Investigate the Underlying Mechanisms in Alzheimer's Disease. *Frontiers in Cellular Neuroscience.* **11**, 291 (2017).
23. Cho, S., Wood, A., & Bowlby, M. R. Brain slices as models for neurodegenerative disease and screening platforms to identify novel therapeutics. *Current neuropharmacology.* **5** (1), 19-33 at <http://www.ncbi.nlm.nih.gov/pubmed/18615151> (2007).
24. Humpel, C. Organotypic brain slice cultures: A review. *Neuroscience.* **305**, 86-98 (2015).
25. Sakmann, B., & Neher, E. Patch clamp techniques for studying ionic channels in excitable membranes. *Annual review of physiology.* **46**, 455-472 (1984).
26. Jensen, M. S., Lambert, J. D. C., & Johansen, F. F. Electrophysiological recordings from rat hippocampus slices following in vivo brain ischemia. *Brain Research.* **554** (1-2), 166-175 (1991).
27. Ferrati, G., Martini, F. J., & Maravall, M. Presynaptic Adenosine Receptor-Mediated Regulation of Diverse Thalamocortical Short-Term Plasticity in the Mouse Whisker Pathway. *Frontiers in Neural Circuits.* **10** (February), 1-9 (2016).
28. Grinvald, A., & Hildesheim, R. VSDI: a new era in functional imaging of cortical dynamics. *Nature Reviews Neuroscience.* **5** (11), 874-885 (2004).
29. Badin, A. S., John, E., & Susan, G. High-resolution spatio-temporal bioactivity of a novel peptide revealed by optical imaging in rat orbitofrontal cortex in vitro: Possible implications for neurodegenerative diseases. *Neuropharmacology.* **73**, 10-18 (2013).
30. Greenfield, S. A., Badin, A. S., Ferrati, G., & Devonshire, I. M. Optical imaging of the rat brain suggests a previously missing link between top-down and bottom-up nervous system function. *Neurophotonics.* **4** (2329-423X (Print)), 31213 (2017).
31. Opitz-Araya, X., & Barria, A. Organotypic hippocampal slice cultures. *Journal of visualized experiments: JoVE.* (48) (2011).
32. Gong, C.-X., Lidsky, T., Wegiel, J., Grundke-Iqbal, I., & Iqbal, K. Metabolically active rat brain slices as a model to study the regulation of protein phosphorylation in mammalian brain. *Brain Research Protocols.* **6** (3), 134-140 (2001).

